Hindawi
Mathematical Problems in Engineering
Volume 2019, Article ID 9026187, 16 pages
https://doi.org/10.1155/2019/9026187

Research Article

A Class of Trigonometric Bernstein-Type Basis Functions with Four Shape Parameters

Yuanpeng Zhu [1] **and Zhuo Liu** [2]

[1] *School of Mathematics, South China University of Technology, Guangzhou, 510641, China*
[2] *Tianan Hi-Tech Ecological Park, Panyu District, Guangzhou 511400, China*

Correspondence should be addressed to Yuanpeng Zhu; ypzhu@scut.edu.cn

Received 24 October 2018; Revised 3 December 2018; Accepted 1 April 2019; Published 17 April 2019

Academic Editor: Nhon Nguyen-Thanh

In this work, a family of four new trigonometric Bernstein-type basis functions with four shape parameters is constructed, which form a normalized basis with optimal total positivity. Based on the new basis functions, a kind of trigonometric Bézier-type curves with four shape parameters, analogous to the cubic Bézier curves, is constructed. With appropriate choices of control points and shape parameters, the resulting trigonometric Bézier-type curves can represent exactly any arc of an ellipse or parabola. The four shape parameters have tension control roles on adjusting the shape of resulting curves. Moreover, a new corner cutting algorithm is also proposed for calculating the trigonometric Bézier-type curves stably and efficiently.

1. Introduction

In computer aided geometric design and computer graphics, parametric curves and surfaces are often expressed by linearly combining control points and basis functions. Generally speaking, basis functions with good properties play a vital role in parametric curves and surfaces design. For instance, if the basis functions have partition of unity, nonnegativity, and total positivity, the resulting parametric curves will possess affine invariance property, convex hull property, and variation diminishing property, which are important in curves design. In engineering, the classical B-spline basis functions have been widely applied in modeling parametric curves; see [1, 2]. However, with the fixed knot vectors, the shape of B-spline curves is determined totally by their control points. One may use the weights in the nonuniform rational B-spline curves to modify the shape of the resulting parametric curves; however, rational form may be unstable and its derivatives and integrals are hard to compute.

In order to adjust the shape of the parametric curves flexibly, some basis functions with shape parameters have been proposed; see [3–5]. These methods have a common idea that new basis functions are constructed by incorporating shape parameters into the classical Bézier or B-spline basis functions. In [6, 7], quadratic and cubic trigonometric Bernstein-type basis functions with shape parameters were shown. In [8], a kind of cubic trigonometric Bernstein-type basis functions possessing two shape parameters was presented, which includes the cubic trigonometric Bernstein-type basis functions with a shape parameter given in [6] as a special case. In [9], shape analysis of the cubic trigonometric Bézier-type curve with a shape parameter given in [6] was presented by using the theory of envelop and topological mapping. Later, in [10], the totally positive property of the cubic trigonometric Bernstein-type basis functions with two shape parameters given in [8] was proved, which implies that the cubic trigonometric Bernstein-type basis with two shape parameters is suitable for conformal design. Recently, a class of cubic trigonometric nonuniform B-spline basis functions having a local shape parameter was proposed in [11], which is an extension of the cubic trigonometric nonuniform spline basis functions with a global shape parameter given in [6]. In [12], a class of C-Bézier basis of the space $\mathrm{span}\{1, t, \sin t, \cos t\}$ was constructed, where the length of the interval serves as shape parameter. Later, in [13], geometric interpretation of the change of the shape parameter on C-Bézier curves was given. In [14], it was proved that the critical length

for the span$\{1, t, \sin t, \cos t\}$ is 2π, which implies that in the span$\{1, t, \sin t, \cos t\}$, Extended Complete Chebyshev- (ECC-) system exists only on interval of length less than 2π. Later, in [15], it was shown that this restriction can be overcome by replacing ECC-system with the Canonical Complete Chebyshev- (CCC-) system.

For controlling the parametric curves efficiently, basis functions with tension shape parameters have aroused great interest among the researchers. In [16], a class of polynomial splines with variable degree was constructed in the space spanned by span$\{1, t, (1-t)^p, t^q\}$, in which p and q serve as tension shape parameters. In [17, 18], it was proved that the polynomial splines with variable degree form a Quasi Extended Chebyshev- (QEC-) system. Later, in [19], the approximation power, the existence of a normalized B-basis, and the structure of a degree-raising process for spaces of the form $\{1, t, t^2, \ldots, t^{n-2}, u(t), v(t)\}$ were given. Within the general framework of QEC-system, the dimension elevation algorithm for the space $\{1, t, t^2, \ldots, t^{n-2}, (1-t)^p, t^q\}$ was studied via blossom theory; see [20–23]. Recently, in [24], the total positivity of the polynomial splines with variable degree was proved based on the theory of CCC-systems. The variable degree polynomial splines have been widely used for constructing shape preserving interpolation and approximation splines; see [25–27]. In [28], based on some truncated polynomial functions, the explicit representations of changeable degree spline basis functions were given. In [29], a kind of five trigonometric blending functions with two exponential shape parameters α and β was proposed in the space spanned by span$\{1, \sin t(1-\sin t)^{\alpha-1}, \cos t(1-\cos t)^{\beta-1}, (1-\sin t)^{\alpha}, (1-\cos t)^{\beta}\}$. Later, in [30], a generalization of these five trigonometric blending functions was presented. Some exponential splines and rational splines with tension shape parameters have also developed for curve design, see [31–33] for example. Recently, four trigonometric Bernstein-type basis functions of the space spanned by span$\{1, \sin^2 t, (1-\sin t)^{\alpha}, (1-\cos t)^{\beta}\}$ were constructed in [34], which form a normalized basis with optimal total positivity. In [35], a family of rational trigonometric basis functions with denominator shape parameters of the space spanned by span$\{1, \sin^2 t, (1-\sin t)^2/[1+(\alpha-2)\sin t], (1-\cos t)^2/[1+(\beta-2)\cos t]\}$ was shown.

The purpose of this paper is to present four new trigonometric Bernstein-type basis functions constructed in the space spanned by span$\{1, \sin^2 t, (1-\sin t)^{\alpha}(1-\lambda\sin t), (1-\cos t)^{\beta}(1-\mu\cos t)\}$, which form a normalized optimal totally positive basis and include the bases given in [6–8, 34] as special cases. The parametric curves constructed by this new basis have shape preserving property. The four shape parameters α, β, λ, and μ have tension control property on modifying the shape of parametric curves. Compared with the four polynomial Bernstein-type basis functions with variable degree constructed in the space span$\{1, t, (1-t)^n, t^m\}$ (see [16]), the new constructed trigonometric Bernstein-type basis functions have more computation complexity for the same degree, while any arc of an ellipse or parabola can be represented exactly by using the new trigonometric Bernstein-type basis functions. And compared with the four rational trigonometric basis functions with two denominator shape parameters constructed in the space spanned by span$\{1, \sin^2 t, (1-\sin t)^2/[1+(\alpha-2)\sin t], (1-\cos t)^2/[1+(\beta-2)\cos t]\}$ (see [35]), the new constructed trigonometric Bernstein-type basis functions possess four shape parameters and thus have more flexibility in free-form curves shape design.

The rest of this paper is organized as follows. In Section 2, the construction and properties of the trigonometric Bernstein-type basis functions are given. Section 3 gives the definition and properties of the trigonometric Bézier-type curves. For computing the trigonometric Bézier-type curves stably and efficiently, a new corner cutting algorithm is developed. Comparison between the trigonometric Bézier-type curves and the variable degree Bézier polynomial curves given in [16] is shown. And tensor product Bézier-type patches are also shown. Conclusions are given in Section 4.

2. Trigonometric Bernstein-Type Basis Functions

2.1. Construction of Trigonometric Bernstein-Type Basis Functions. For arbitrary real numbers $\alpha, \beta \in [2, +\infty), \lambda \in (-\alpha, 1], \mu \in (-\beta, 1]$, $t \in [0, \pi/2]$, a new family of trigonometric Bernstein-type basis functions will be constructed in the space

$$T_{\alpha,\beta,\lambda,\mu} := span\left\{1, \sin^2 t, (1-\sin t)^{\alpha} \cdot (1-\lambda\sin t), (1-\cos t)^{\beta}(1-\mu\cos t)\right\}. \tag{1}$$

The corresponding mother-function is given as follows:

$$\Phi(t) := \left(\sin^2 t, (1-\sin t)^{\alpha}(1-\lambda\sin t), (1-\cos t)^{\beta} \cdot (1-\mu\cos t)\right), \quad t \in \left[0, \frac{\pi}{2}\right]. \tag{2}$$

We shall prove the totally positive property of the new basis functions by using the theory of Quasi Extended Chebyshev (QEC) space. The related concepts concerning ECC-space, QEC-space, blossom, and Quasi Bernstein-type basis can be found in [17, 18, 20–23, 34].

In the following theorem, we will show that the following space

$$DT_{\alpha,\beta,\lambda,\mu} := span\left\{2\sin t\cos t, -\cos t(1-\sin t)^{\alpha-1} \cdot [\alpha(1-\lambda\sin t) + \lambda(1-\sin t)], \sin t(1-\cos t)^{\beta-1} \cdot [\beta(1-\mu\cos t) + \mu(1-\cos t)]\right\} \tag{3}$$

is a 3-dimensional QEC-space on $t \in [0, \pi/2]$.

Theorem 1. *For any real numbers $\alpha, \beta \in [2, +\infty), \lambda \in (-\alpha, 1], \mu \in (-\beta, 1]$, the space $T_{\alpha,\beta,\lambda,\mu}$ is a 3-dimensional QEC-space on $[0, \pi/2]$.*

Proof. For any $\xi_i \in \mathbb{R}$, $t \in [0, \pi/2]$, we consider a linear combination

$$\begin{aligned}&\xi_0 (2\sin t\cos t)\\&-\xi_1\cos t(1-\sin t)^{\alpha-1}[\alpha(1-\lambda\sin t)+\lambda(1-\sin t)]\\&+\xi_2\sin t(1-\cos t)^{\beta-1}[\beta(1-\mu\cos t)+\mu(1-\cos t)]\\&=0.\end{aligned}\tag{4}$$

From (4), for $t=0$ and $t=\pi/2$, we have $\xi_1=0$ and $\xi_2=0$, respectively. It follows that $\xi_0=0$. Thus we can see that the space $DT_{\alpha,\beta,\lambda,\mu}$ is a 3-dimensional space.

We will prove that the space $DT_{\alpha,\beta,\lambda,\mu}$ forms a QEC-space on $[0,\pi/2]$ by two steps. In the first step, we prove that the space $DT_{\alpha,\beta,\lambda,\mu}$ forms an ECC-space in $(0,\pi/2)$. For any $t\in[a,b]\subset(0,\pi/2)$, let

$$\begin{aligned}u(t)&=\left[\frac{-\alpha(1-\sin t)^{\alpha-1}(1-\lambda\sin t)-\lambda(1-\sin t)^{\alpha}}{\sin t}\right]'\\&=\frac{\cos t(1-\sin t)^{\alpha-2}\left[\alpha+\lambda+(\alpha+\lambda)(\alpha-2)\sin t+\lambda\left(1-\alpha^2\right)\sin^2 t\right]}{\sin^2 t},\end{aligned}\tag{5}$$

and

$$\begin{aligned}v(t)&=\left[\frac{\beta(1-\cos t)^{\beta-1}(1-\mu\cos t)+\mu(1-\cos t)^{\beta}}{\cos t}\right]'\\&=\frac{\sin t(1-\cos t)^{\beta-2}\left[\beta+\mu+(\beta+\mu)(\beta-2)\cos t+\mu\left(1-\beta^2\right)\cos^2 t\right]}{\cos^2 t}.\end{aligned}\tag{6}$$

Both the two functions $u(t)$ and $v(t)$ are positive on any subinterval $[a,b]\subset(0,\pi/2)$. In fact, for $A\in[2,+\infty)$, $B\in(-A,1]$ and $x\in(0,1)$, consider the following quadratic function:

$$Q(x)=A+B+(A+B)(A-2)x+B\left(1-A^2\right)x^2.\tag{7}$$

For $A\in[2,+\infty)$, $B\in(0,1]$, notice that $B(1-A^2)<0$; we have

$$\begin{aligned}\min_{x\in(0,1)}Q(x)&>\min\{Q(0),Q(1)\}\\&=\min\{A+B,(1-B)A(A-1)\}>0.\end{aligned}\tag{8}$$

Furthermore, for $A\in[2,+\infty)$, $B\in(-A,0]$, $x\in(0,1)$, direct computation gives that

$$\begin{aligned}Q'(x)&=(A+B)(A-2)+2B\left(1-A^2\right)x>Q'(0)\\&=(A+B)(B-2)\geq 0.\end{aligned}\tag{9}$$

From this together with $Q(0)=A+B>0$, we can see that $Q(x)>0$ for any $x\in(0,1)$. These imply that $Q(x)>0$ for any $A\in[2,+\infty)$, $B\in(-A,1]$ and $x\in(0,1)$. Thus we can see that $u(t)>0$ and $v(t)>0$ for any $t\in[a,b]\subset(0,\pi/2)$.

For $\alpha,\beta\in[2,+\infty)$, $\lambda\in(-\alpha,1]$, $\mu\in(-\beta,1]$, by directly computing, we get

$$\begin{aligned}u'(t)=&-\frac{1}{\sin^3 t}\left\{\sin^2 t(1-\sin t)^{\alpha-1}\right.\\&\cdot[\lambda(1-\sin t)+\alpha(1-\lambda\sin t)]\\&+\alpha\sin^3 t(1-\sin t)^{\alpha-2}\\&\cdot[2\lambda(1-\sin t)+(\alpha-1)(1-\lambda\sin t)]+\alpha(\alpha-1)\\&\cdot\sin^2 t\cos^2 t(1-\sin t)^{\alpha-3}\\&\cdot[3\lambda(1-\sin t)+(\alpha-2)(1-\lambda\sin t)]+2\alpha\sin t\\&\cdot\cos^2 t(1-\sin t)^{\alpha-2}\\&\cdot[2\lambda(1-\sin t)+(\alpha-1)(1-\lambda\sin t)]\\&+2\cos^2 t(1-\sin t)^{\alpha-1}\\&\left.\cdot[\lambda(1-\sin t)+\alpha(1-\lambda\sin t)]\right\}<0,\\v'(t)=&\frac{1}{\cos^3 t}\left\{\cos^2 t(1-\cos t)^{\beta-1}\right.\\&\cdot\left[\mu(1-\cos t)+\beta(1-\mu\cos t)\right]+\beta\cos t^3\\&\cdot(1-\cos t)^{\beta-2}\\&\left.\cdot\left[2\mu(1-\cos t)+(\beta-1)(1-\mu\cos t)\right]\right.\end{aligned}$$

$$+\beta(\beta-1)\sin^2 t\cos^2 t(1-\cos t)^{\beta-3}\cdot[3\mu(1-\cos t)+(\beta-2)(1-\mu\cos t)]+2\beta\sin^2 t\cdot\cos t(1-\cos t)^{\beta-2}\cdot[2\mu(1-\cos t)+(\beta-1)(\mu\cos t-1)]+2\sin^2 t\cdot\cos t(1-\cos t)^{\beta-1}\cdot[\mu(1-\cos t)+\beta(1-\mu\cos t)]\}>0. \tag{10}$$

It follows that the Wronskian of $u(t)$ and $v(t)$ is positive in $[a,b]$, that is,

$$W(u,v)(t)=u(t)v'(t)-u'(t)v(t)>0,\quad \forall t\in[a,b]. \tag{11}$$

For any $A>0$, $B>0$, $C>0$, and $t\in[a,b]$, we consider the following three weight functions:

$$w_0(t)=2\sin t\cos t,\quad w_1(t)=Au(t)+Bv(t),\quad w_2(t)=C\frac{W(u,v)(t)}{[Au(t)+Bv(t)]^2}. \tag{12}$$

Obviously, all the three weight functions $w_i(t)$, $i=0,1,2$ are C^∞, positive and bounded on $[a,b]$. For the following ECC-space defined by the three weight functions $w_i(t)$, $i=0,1,2$,

$$u_0(t)=w_0(t),\quad u_1(t)=w_0(t)\int_a^t w_1(t_1)\,dt_1,\quad u_2(t)=w_0(t)\int_a^t w_1(t_1)\int_a^{t_1} w_2(t_2)\,dt_2\,dt_1, \tag{13}$$

after some simple computation, we can see that all the three functions $u_0(t)$, $u_1(t)$, and $u_2(t)$ can be expressed as the forms of some linear combinations of the three functions $2\sin t\cos t$, $-\cos t(1-\sin t)^{\alpha-1}[\alpha(1-\lambda\sin t)+\lambda(1-\sin t)]$, $\sin t(1-\cos t)^{\beta-1}[\beta(1-\mu\cos t)+\mu(1-\cos t)]$, which implies that the space $DT_{\alpha,\beta,\lambda,\mu}$ is an ECC-space on $[a,b]$. Since $[a,b]$ are arbitrary subinterval of $(0,\pi/2)$, we can further conclude that the space $DT_{\alpha,\beta,\lambda,\mu}$ is an ECC-space in $(0,\pi/2)$.

In the second step, we further prove that the space $DT_{\alpha,\beta,\lambda,\mu}$ forms a QEC-space on $[0,\pi/2]$. To this end, we need to prove that any nonzero element of the space $DT_{\alpha,\beta,\lambda,\mu}$ has at most 2 roots on $[0,\pi/2]$ (keep it in mind that in a QEC-space, we count multiplicities as far as possible up to 2). Consider any nonzero function

$$G(t)=C_0[2\sin t\cos t]+C_1\{-\cos t(1-\sin t)^{\alpha-1}\cdot[\alpha(1-\lambda\sin t)+\lambda(1-\sin t)]\}+C_2\{\sin t\cdot(1-\cos t)^{\beta-1}[\beta(1-\mu\cos t)+\mu(1-\cos t)]\}, \tag{14}$$

where $t\in[0,\pi/2]$. Since the space $DT_{\alpha,\beta,\lambda,\mu}$ is an ECC-space in $(0,\pi/2)$, $G(t)$ has at most two roots in $(0,\pi/2)$. Suppose that the function $G(t)$ has a root at 0; then we get $C_1=0$. In this case, if $C_2=0$, then $G(t)$ has a singular root at 0 and a singular root at $\pi/2$. If $C_0=0$, we can check that 0 is a double root of $G(t)$ (we count multiplicities as far as possible up to 2). If $C_0C_2>0$, $G(t)$ has singular one root at 0 and it does not vanish anywhere on $(0,\pi/2]$. If $C_0C_2<0$, $G(t)$ has singular one root at 0 and it does not vanish at $\pi/2$. Moreover, for the following function

$$K(t)\coloneqq 2C_0\cos t+C_2(1-\cos t)^{\beta-1}\cdot[\beta(1-\mu\cos t)+\mu(1-\cos t)], \tag{15}$$

by directly computing, we obtain

$$K'(t)=-2C_0\sin t+C_2\beta\sin t(1-\cos t)^{\beta-2}\cdot[\mu(\beta+1)(1-\cos t)+(\beta-1)(1-\mu\cos t)]\geq 0, \tag{16}$$

and it follows that $K(t)$ is a monotone increasing function on $[0,\pi/2]$. From these together with $K(0)K(\pi/2)=2C_0C_2(\beta+\mu)<0$, we can see that $K(t)$ has exactly singular one root in $(0,\pi/2)$; thus we can immediately conclude that $G(t)=\sin tK(t)$ (notice that $C_1=0$ for the current case) has exactly one root in $(0,\pi/2)$. Similarly, for the case that $G(t)$ has a root at $\pi/2$, we can also derive that the function $G(t)$ has at most 2 roots on $[0,\pi/2]$ (we count multiplicities as far as possible up to 2). Summarizing the above analysis, we can conclude that the space $DT_{\alpha,\beta}$ is a QEC-space on $[0,\pi/2]$. □

Since the space $DT_{\alpha,\beta,\lambda,\mu}$ forms a QEC-space on $[0,\pi/2]$, from Theorem 3.1 of [21], we can conclude that blossom exists in $T_{\alpha,\beta,\lambda,\mu}$, which indicates that the new space $T_{\alpha,\beta,\lambda,\mu}$ is suited for curve design. In addition, from Theorem 2.18 of [21], we can also know that the space $T_{\alpha,\beta,\lambda,\mu}$ has a normalized basis of Quasi Bernstein-type on $[0,\pi/2]$. In the next Theorem 3, we will compute the associated Chebyshev-Bézier points of the mother-function $\Phi(t)$ defined in (2) and construct the associated trigonometric Bernstein-type basis $T_i\coloneqq T_i^{(0,\pi/2)}$ of the space $T_{\alpha,\beta,\lambda,\mu}$. Before further discussion, we want to prove the following lemma, which will be used to discuss the positivity of the trigonometric Bernstein-type basis.

Lemma 2. *For any $x\in[0,1]$, $y\in[1,+\infty)$, the function $f(x,y)=1-x^2-(1-x)^y(1+xy)\geq 0$.*

Proof. For any $x\in[0,1]$, $y\in[1,+\infty)$, direct computation that $f(0,y)=0$, $f(1,y)=0$, and $f(x,1)=0$. For any $x\in(0,1)$, the function $g(x)=x+\ln(1-x)<0$. In fact, $g'(x)=x/(x-1)<0$ and $g(0)=0$. Therefore, for $x\in[0,1]$, $y\in[1,+\infty)$, we have

$$\frac{\partial f(x,y)}{\partial y}=-(1-x)^y\{[x+\ln(1-x)]+xy\ln(1-x)\}>0, \tag{17}$$

Thus $f(x,y)$ increases with the increase of y for any fixed $x\in(0,1)$. From these, for any $x\in(0,1)$, $y\in[1,+\infty)$, we have $f(x,y)\geq f(x,1)=0$. □

Theorem 3. *For any $\alpha, \beta \in [2, +\infty), \lambda \in (-\alpha, 1], \mu \in (-\beta, 1]$, the four Chebyshev-Bézier points $\Pi_i := \Pi_i(0, \pi/2)$ of the mother-function $\Phi(t)$ defined in (2) are given by*

$$\begin{aligned} \Pi_0 &= (0, 1, 0), \\ \Pi_1 &= (0, 0, 0), \\ \Pi_2 &= (1, 0, 0), \\ \Pi_3 &= (1, 0, 1). \end{aligned} \tag{18}$$

The four associated trigonometric Bernstein-type (TB-type for short) basis functions of the space $T_{\alpha,\beta,\lambda,\mu}$ are given by

$$\begin{aligned} T_0(t) &= (1 - \sin t)^{\alpha} (1 - \lambda \sin t), \\ T_1(t) &= 1 - \sin^2 t - (1 - \sin t)^{\alpha} (1 - \lambda \sin t), \\ T_2(t) &= 1 - \cos^2 t - (1 - \cos t)^{\beta} (1 - \mu \cos t), \\ T_3(t) &= (1 - \cos t)^{\beta} (1 - \mu \cos t). \end{aligned} \tag{19}$$

And the system of functions $(T_0(t), T_1(t), T_2(t), T_3(t))$ forms a normalized basis of the space $T_{\alpha,\beta,\lambda,\mu}$ with optimal total positivity.

Proof. For arbitrary $\alpha, \beta \in [2, +\infty), \lambda \in (-\alpha, 1], \mu \in (-\beta, 1]$, from the expression of the mother-function $\Phi(t)$ given in (2), we get

$$\begin{aligned} \Phi(0) &= (0, 1, 0), \\ \Phi\left(\frac{\pi}{2}\right) &= (1, 0, 1), \\ \Phi'(0) &= (0, -\alpha - \lambda, 0), \\ \Phi'\left(\frac{\pi}{2}\right) &= (0, 0, \beta + \mu), \\ \Phi''(0) &= \left(2, \alpha^2 + 2\lambda\alpha - \alpha, 0\right), \\ \Phi''\left(\frac{\pi}{2}\right) &= \left(-2, 0, \beta^2 + 2\mu\beta - \beta\right). \end{aligned} \tag{20}$$

Thus, by simply computing, we get

$$\begin{aligned} \Pi_0 &= \Phi(0) = (0, 1, 0), \\ \Pi_3 &= \Phi(1) = (1, 0, 1), \\ \{\Pi_1\} &= \mathrm{Osc}_1 \Phi(0) \cap \mathrm{Osc}_2 \Phi(1) = (0, 0, 0), \\ \{\Pi_2\} &= \mathrm{Osc}_2 \Phi(0) \cap \mathrm{Osc}_1 \Phi(1) = (1, 0, 0). \end{aligned} \tag{21}$$

For any $t \in [0, \pi/2]$, from $\Phi(t) = \sum_{i=0}^{3} T_i(t) \Pi_i$, we have

$$\begin{aligned} T_2(t) + T_3(t) &= \sin^2 t, \\ T_0(t) &= (1 - \sin t)^{\alpha} (1 - \lambda \sin t), \\ T_3(t) &= (1 - \cos t)^{\beta} (1 - \mu \cos t). \end{aligned} \tag{22}$$

Therefore, from (22) together with $\sum_{i=0}^{3} T_i(t) = 1$, we can easily derive the expressions of the new basis functions $T_i(t)$, $i = 0, 1, 2, 3$.

It can be easily checked that the new basis functions have the following important end-point property.

(i) $T_0(0) = 1$, and $T_0(t)$ vanishes 3 times at $\pi/2$ (we count multiplicities as far as possible up to 3).

(ii) $T_3(\pi/2) = 1$, and $T_3(t)$ vanishes 3 times at 0 (we count multiplicities as far as possible up to 3).

(iii) For $i = 1, 2$, $T_i(t)$ vanishes exactly i times at 0 and exactly $(3 - i)$ times at $\pi/2$.

For any $\alpha, \beta \in [2, +\infty), \lambda \in (-\alpha, 1], \mu \in (-\beta, 1]$, $t \in [0, \pi/2]$, it is obvious that $T_i(t) \geq 0$ $(i = 0, 3)$. And for $T_1(t)$, $T_2(t)$, by using the Lemma 2, we have

$$\begin{aligned} T_1(t) &= 1 - \sin^2 t - (1 - \sin t)^{\alpha} (1 - \lambda \sin t) \\ &\geq 1 - \sin^2 t - (1 - \sin t)^{\alpha} (1 + \alpha \sin t) \geq 0. \\ T_2(t) &= 1 - \cos^2 t - (1 - \cos t)^{\alpha} (1 - \mu \cos t) \\ &\geq 1 - \cos^2 t - (1 - \cos t)^{\beta} (1 + \beta \cos t) \geq 0. \end{aligned} \tag{23}$$

In addition, for each $0 \leq i \leq 3$, the function $T_i(t)$ is strictly positive in $(0, \pi/2)$. Thus, from Definition 2.10 of [21], we can see that the normalized trigonometric Bernstein-type basis (19) is precisely the Quasi Bernstein-type basis of the space $T_{\alpha,\beta,\lambda,\mu}$. Moreover, from Theorem 2.18 of [21], we can conclude that the normalized trigonometric Bernstein-type basis (19) is exactly the normalized basis of the space $T_{\alpha,\beta,\lambda,\mu}$ restricted to $[0, \pi/2]$ with optimal total positivity. □

Remark 4. It is easy to check that, for $\alpha = \beta = 2$, $\lambda = \mu$, the four TB-type basis functions (19) will return to the four TB-type basis functions with a shape parameter given in [6]. For $\alpha = \beta = 1$, the four TB-type basis functions (19) will return to the four TB-type basis functions with two shape parameters given in [7]. And for $\alpha = \beta = 2$, the four TB-type basis functions (19) will return to the four TB-type basis functions with two shape parameters given in [8]. Moreover, for $\lambda = \mu = 0$, the four TB-type basis functions (19) will return to the four TB-type basis functions with two exponential shape parameters given in [34].

From Lemma 2, it is easy to see that for $\alpha, \beta \in [1, +\infty), \lambda \in (-\alpha, 1], \mu \in (-\beta, 1]$, the four TB-type basis functions (19) also satisfy $T_i(t) \geq 0$ for any $t \in [0, \pi/2]$.

For convenience, we shall also denote the four TB-type basis functions as $T_i(t; \alpha, \beta, \lambda, \mu)$, $i = 0, 1, 2, 3$, or $T_i(t; \alpha, \lambda)$, $i = 0, 1$, $T_i(t; \beta, \mu)$, $i = 2, 3$. Figure 1 shows some TB-type basis functions with different shape parameters.

3. Construction of the Trigonometric Bézier-Type Curves

Definition 5. Given control points P_i $(i = 0, 1, 2, 3)$ in $\mathbb{R}^2$ or $\mathbb{R}^3$, and $\alpha, \beta \in [2, +\infty), \lambda \in (-\alpha, 1], \mu \in (-\beta, 1]$ then

$$T(t; \alpha, \beta, \lambda, \mu) = \sum_{i=0}^{3} T_i(t; \alpha, \beta, \lambda, \mu) P_i, \quad t \in \left[0, \frac{\pi}{2}\right] \tag{24}$$

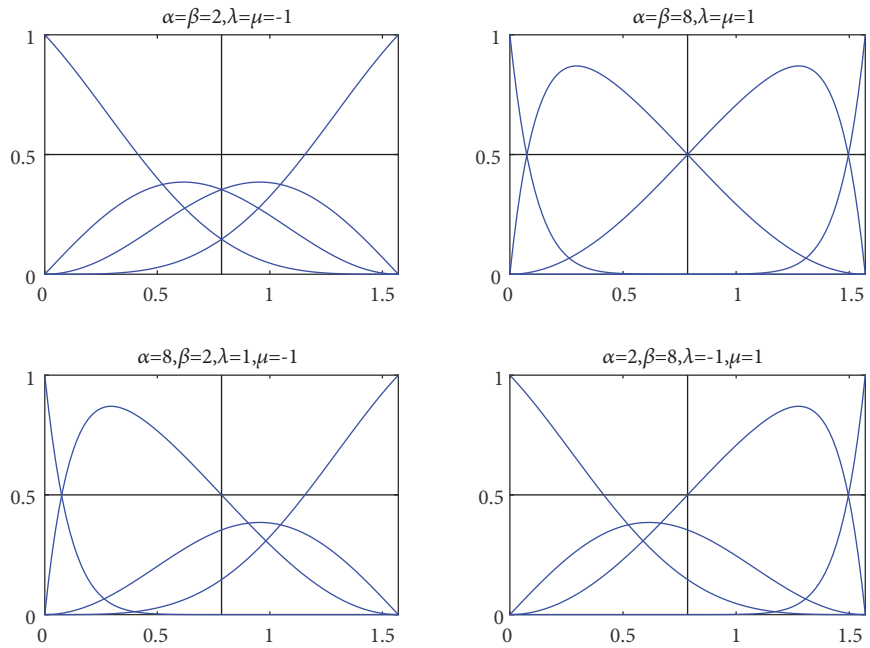

Figure 1: TB-type basis functions with different shape parameters.

is called a trigonometric Bézier-type (TB-type for short) curve with four shape parameters α, β, λ, and μ.

Since the TB-type basis functions given in (19) possess the properties including partition of unity, nonnegativity, and total positivity, the corresponding TB-type curves given in (24) have the corresponding properties of affine invariance, convex hull, and variation diminishing, which are crucial in curve design. For any $\alpha, \beta \in [2, +\infty)$, $\lambda \in (-\alpha, 1]$, $\mu \in (-\beta, 1]$, after some direct computation, we can obtain the following end-point property of the TB-type curve

$$\begin{aligned}
&T(0;\alpha,\beta,\lambda,\mu) = P_0,\\
&T\left(\frac{\pi}{2};\alpha,\beta,\lambda,\mu\right) = P_3,\\
&T'(0;\alpha,\beta,\lambda,\mu) = (\alpha+\lambda)(P_1-P_0),\\
&T'\left(\frac{\pi}{2};\alpha,\beta,\lambda,\mu\right) = (\beta+\mu)(P_3-P_2),\\
&T''(0;\alpha,\beta,\lambda,\mu)\\
&\quad = \left(\alpha^2+2\lambda\alpha-\alpha\right)(P_0-P_1)+2(P_2-P_1),\\
&T''\left(\frac{\pi}{2};\alpha,\beta,\lambda,\mu\right)\\
&\quad = \left(\beta^2+2\mu\beta-\beta\right)(P_3-P_2)+2(P_1-P_2),\\
&T'''(0;\alpha,\beta,\lambda,\mu)\\
&\quad = \left[\alpha^3+3(\lambda-1)\alpha^2-3\lambda\alpha+\alpha-\lambda\right](P_1-P_0),\\
&T'''\left(\frac{\pi}{2};\alpha,\beta,\lambda,\mu\right)\\
&\quad = \left(\beta^3+3(\mu-1)\beta^2-3\mu\beta+\beta-\mu\right)(P_3-P_2).
\end{aligned} \tag{25}$$

The above listed end-point property indicates that for arbitrary $\alpha, \beta \in [2, +\infty)$, the TB-type curve has end-point interpolation property and the tangent lines of the TB-type curve at the points P_0 and P_3 are P_0P_1, P_2P_3, respectively. Therefore, we can see that the TB-type curve has some similar properties to that of the classical cubic Bézier curve.

3.1. Shape Control and Corner Cutting Algorithm. For $t \in [0, \pi/2]$, we rewrite the expression of the TB-type curve (24) as the following form:

$$\begin{aligned}
T(t;\alpha,\beta,\lambda,\mu) = {} & \cos^2 t P_1 + \sin^2 t P_2\\
& + T_0(t;\alpha,\lambda)(P_0-P_1)\\
& + T_3(t;\beta,\mu)(P_3-P_2).
\end{aligned} \tag{26}$$

Obviously, $T_0(t;\alpha,\lambda)$ decreases with the increase of α or λ for any fixed $t \in (0, \pi/2)$. This implies that the resulting TB-type curve moves in the same direction of the edge $P_0 - P_1$ as α or λ increases. On the contrary, when α or λ decreases, the resulting TB-type curve will move in the opposite direction to the edge $P_0 - P_1$. The shape parameters β and μ have the similar effects on the edge $P_3 - P_2$. As α, λ or β, μ increase, respectively, the TB-type curve will tend to the point P_1 or P_2, respectively. And when the shape parameters satisfy $\alpha = \beta$, $\lambda = \mu$, the TB-type curve will move in the same direction or the opposite direction to the edge $P_2 - P_1$ when α or λ increases or decreases, respectively. These imply that the four shape parameters α, λ, β, and μ serve as local tension parameters. Figures 2 and 3 give some examples that the shape of TB-type curves can be modified conveniently by using the four shape parameters under the fixed control points.

For computing the proposed TB-type curves efficiently and stably, we shall develop a new corner cutting algorithm,

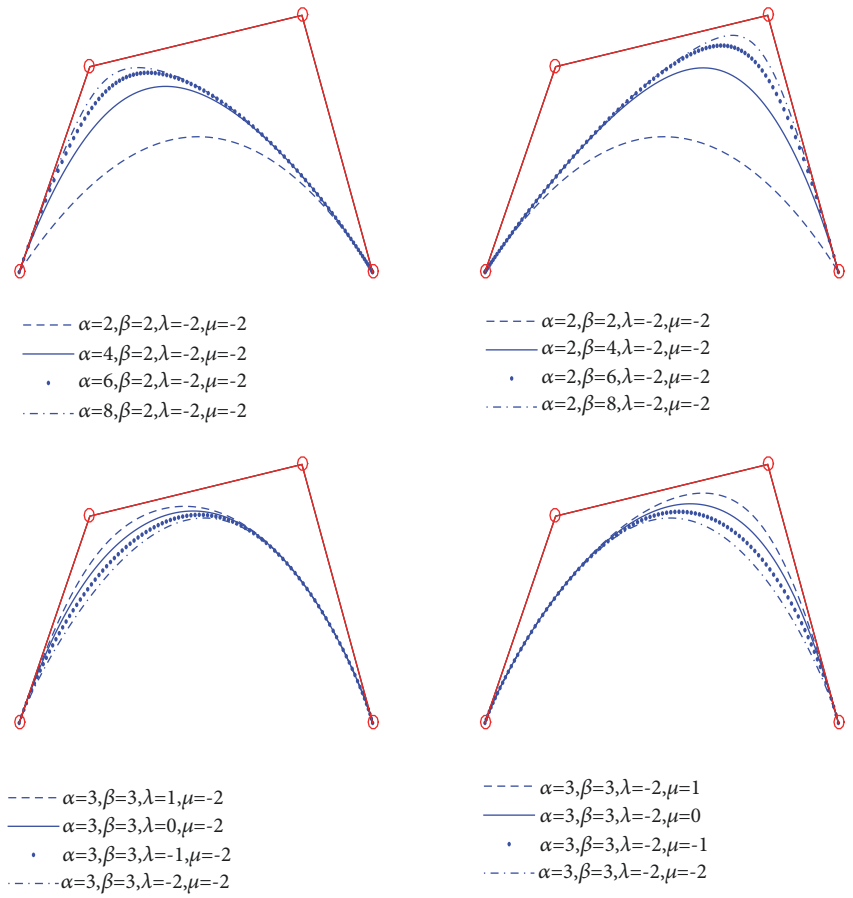

Figure 2: The effect of the shape parameters on the TB-type curves.

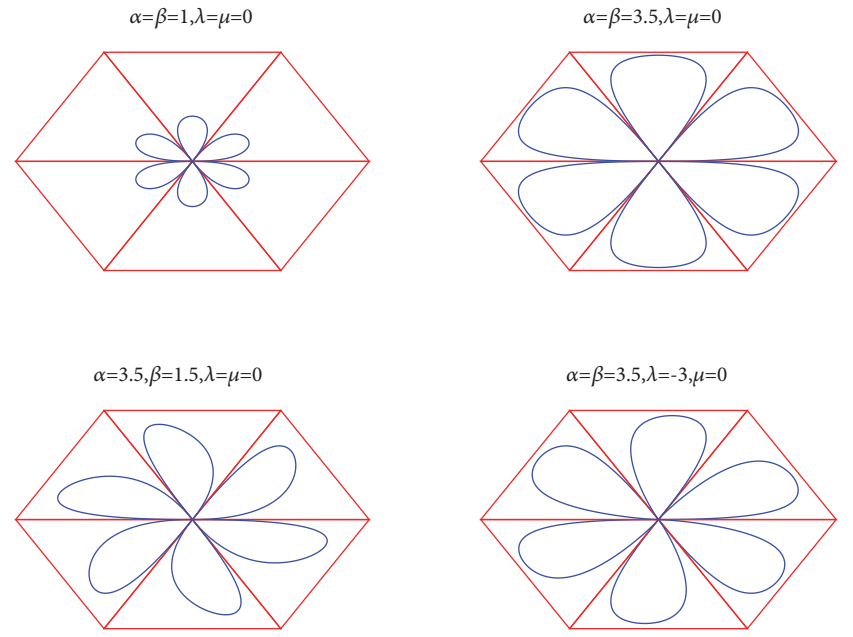

Figure 3: The effect of the shape parameters on the TB-type curves.

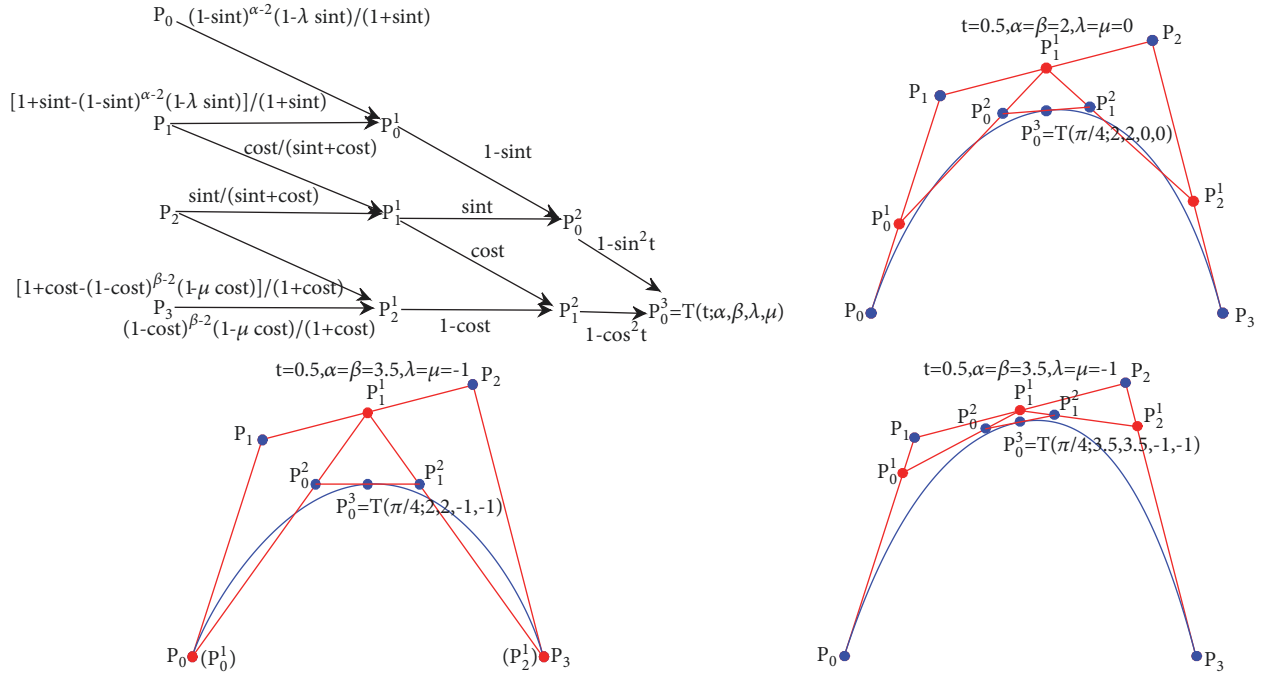

FIGURE 4: Corner cutting algorithm with different shape parameters.

which is formed by convex combinations. For this purpose, we further rewrite the TB-type curve (24) into the following matrix multiplication form:

$$T(t;\alpha,\beta;\lambda,\mu) = \left(1-\sin^2 t \quad 1-\cos^2 t\right) \times \begin{pmatrix} 1-\sin t & \sin t & 0 \\ 0 & \cos t & 1-\cos t \end{pmatrix} \times \begin{pmatrix} E_1(t) & E_2(t) & 0 & 0 \\ 0 & E_3(t) & E_4(t) & 0 \\ 0 & 0 & E_5(t) & E_6(t) \end{pmatrix} \times \begin{pmatrix} P_0 \\ P_1 \\ P_2 \\ P_3 \end{pmatrix}, \tag{27}$$

where

$$E_1(t) = \frac{(1-\sin t)^{\alpha-2}(1-\lambda \sin t)}{1+\sin t},$$

$$E_2(t) = \frac{\left[1+\sin t-(1-\sin t)^{\alpha-2}(1-\lambda \sin t)\right]}{1+\sin t},$$

$$E_3(t) = \frac{\cos t}{\sin t+\cos t},$$

$$E_4(t) = \frac{\sin t}{\sin t+\cos t},$$

$$E_5(t) = \frac{\left[1+\cos t-(1-\cos t)^{\beta-2}(1-\mu \cos t)\right]}{1+\cos t},$$

$$E_6(t) = \frac{(1-\cos t)^{\beta-2}(1-\mu \cos t)}{1+\cos t}. \tag{28}$$

It is easy to check that $E_1(t) + E_2(t) = 1$, $E_3(t) + E_4(t) = 1$, and $E_5(t) + E_6(t) = 1$. Thus (27) provides a new corner cutting algorithm for computing the proposed TB-type curve (24). Figure 4 gives some examples of this new algorithm with different shape parameters.

3.2. The Representation of Elliptic and Parabolic Arcs. In this subsection, we shall show that with appropriated choices of control points and shape parameters, any arc of an ellipse or parabola can be represented exactly by using the new TB-type curves $T(t;\alpha,\beta,\lambda,\mu)$ given in (24).

For $\alpha = \beta = 1$, $\lambda = \mu = 0$, if the control points are $P_0 = (x_0+a, y_0)$, $P_1 = (x_0+a, y_0+b)$, $P_2 = (x_0+a, y_0+b)$, $P_3 = (x_0, y_0+b)$, then the coordinates of the generated TB-type curve $T(t;1,1,0,0)$ are

$$x(t) = x_0 + a\cos t$$
$$y(t) = y_0 + b\sin t, \qquad t \in \left[0, \frac{\pi}{2}\right]. \tag{29}$$

This expression shows that $T(t;1,1,0,0)$ is a quarter of elliptic arc whose center locates at (x_0, y_0). By constraining the parameter t on the desired interval $[\theta_1, \theta_2]$, we can obtain an

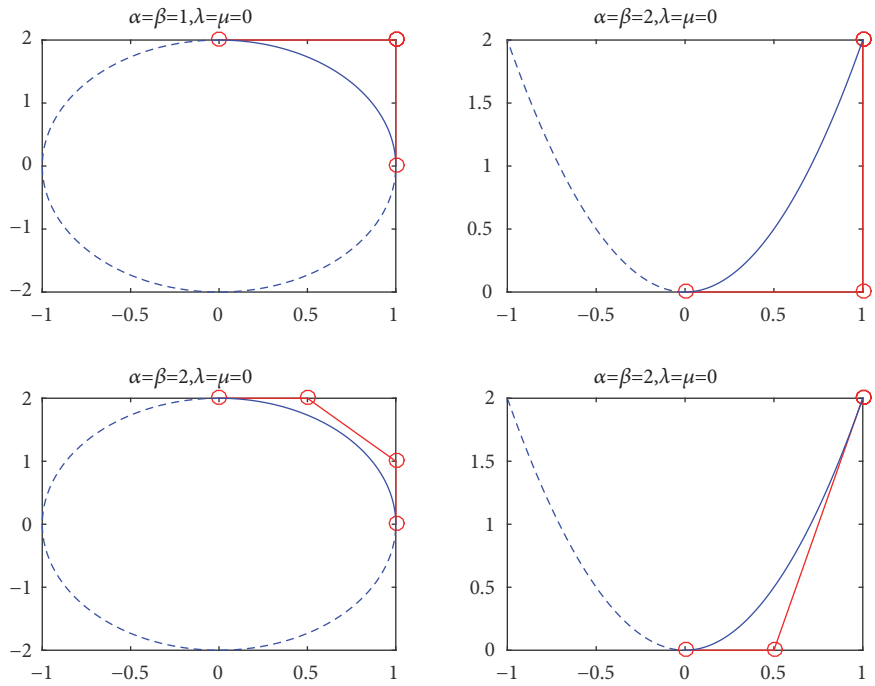

Figure 5: The representation of elliptic and parabolic arcs.

arc of an ellipse whose starting angle and ending angle are θ_1 and θ_2, respectively.

And for $\alpha = \beta = 1, \lambda = \mu = 1, b - a > 0$, if we set the control points as $P_0 = (a, c_2a^2 + c_1a + c_0)$, $P_1 = (b, 2c_2ab - c_2a^2 + c_1b + c_0)$, $P_2 = (b, c_2b^2 + c_1b + c_0)$, $P_3 = (b, c_2b^2 + c_1b + c_0)$, then from (24) we have the corresponding coordinates of $T(t; 1, 1, 0, 0)$ as follows:

$$\begin{aligned} x(t) &= (b-a)\sin t + a \\ y(t) &= c_2\left[(b-a)\sin t + a\right]^2 + c_1\left[(b-a)\sin t + a\right] \\ &\quad + c_0, \\ &\qquad t \in \left[0, \frac{\pi}{2}\right]. \end{aligned} \tag{30}$$

The result indicates that the $T(t; 1, 1, 0, 0)$ is a segment of the parabola $y = c_2x^2 + c_1x + c_0$, $x \in [a, b]$.

For $\alpha = \beta = 2$, $\lambda = \mu = 0$, if the control points are $P_0 = (x_0 + a, y_0)$, $P_1 = (x_0 + a, y_0 + b/2)$, $P_2 = (x_0 + a/2, y_0 + b)$, and $P_3 = (x_0, y_0 + b)$, then the coordinates of the generated curve $T(t; 2, 2, 0, 0)$ are

$$\begin{aligned} x(t) &= x_0 + a\cos t \\ y(t) &= y_0 + b\sin t, \\ &\qquad t \in \left[0, \frac{\pi}{2}\right]. \end{aligned} \tag{31}$$

This expression shows that $T(t; 2, 2, 0, 0)$ is a quarter of elliptic arc whose center locates at (x_0, y_0). By constraining the parameter t on the desired interval $[\theta_1, \theta_2]$, we can obtain an arc of an ellipse whose starting angle and ending angle are θ_1 and θ_2, respectively.

Furthermore, for $\alpha = \beta = 2, \lambda = \mu = 2$, and $b - a > 0$, if the control points P_0, P_1, P_2, and P_3 with respective coordinates $(b, c_2b^2 + c_1b + c_0)$, $(b, c_2b^2 + c_1b + c_0)$, $((b + a)/2, c_2ab + c_1(b + a)/2 + c_0)$, and $(a, c_2a^2 + c_1a + c_0)$, then from (24) we obtain

$$\begin{aligned} x(t) &= (b-a)\cos t + a \\ y(t) &= c_2\left[(b-a)\cos t + a\right]^2 + c_1\left[(b-a)\cos t + a\right] \\ &\quad + c_0, \\ &\qquad t \in \left[0, \frac{\pi}{2}\right], \end{aligned} \tag{32}$$

which gives a segment of the parabola $y = c_2x^2 + c_1x + c_0$, $x \in [a, b]$.

From the above discussion, we can see that the proposed TB-type curves can represent any arc of an ellipse or parabola can be represented exactly. Figure 5 shows some elliptic and parabolic arcs constructed by using the TB-type curves (marked with solid blue lines).

3.3. Approximation. Control polygons provide an important tool in geometric modeling. It is an advantage if the curve being modeled tends to preserve the shape of its control polygon. Now we show some relations of the TB-type curves (24) and the cubic Bézier curves corresponding to their control polygons.

Theorem 6. *Suppose the control points P_0, P_1, P_2, P_3 are not collinear. For $u \in [0, 1]$, the relationships between*

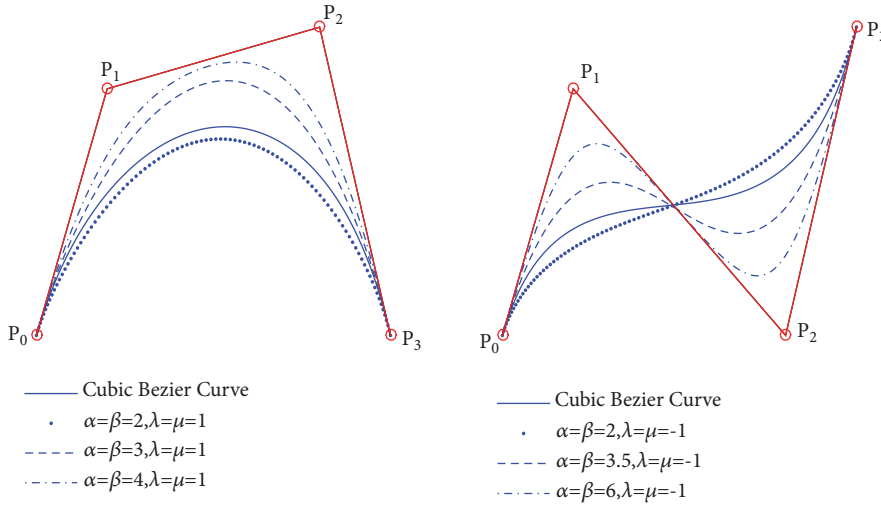

Figure 6: TB-like curves and cubic Bézier curves.

TB-type curve $T((\pi/2)u;\alpha,\beta,\lambda,\mu)$ *and the cubic Bézier curve* $B(u;\alpha,\beta,\lambda,\mu)=\sum_{i=0}^{3}P_iC_3^i(1-u)^{3-i}u^i$ *are as follows:*

$$\begin{aligned}
&T\left(0;\alpha,\beta,\lambda,\mu\right)=B\left(0\right),\\
&T\left(1;\alpha,\beta,\lambda,\mu\right)=B\left(1\right),\\
&T\left(\frac{\pi}{4};\alpha,\beta,\lambda,\mu\right)-P^*\\
&\quad\le h\left(\alpha,\beta,\lambda,\mu\right)\left[B\left(\frac{1}{2}\right)-P^*\right].
\end{aligned}\tag{33}$$

where $P^*=(P_1+P_2)/2$, $h(\alpha,\beta,\lambda,\mu)=\max\{\phi(\alpha,\lambda),\varphi(\beta,\mu)\}$, *and*

$$\begin{aligned}
\phi\left(\alpha,\lambda\right)&=8\left(1-\frac{\sqrt{2}}{2}\right)^{\alpha}\left(1-\lambda\frac{\sqrt{2}}{2}\right),\\
\varphi\left(\beta,\mu\right)&=8\left(1-\frac{\sqrt{2}}{2}\right)^{\beta}\left(1-\mu\frac{\sqrt{2}}{2}\right).
\end{aligned}\tag{34}$$

Proof. By direct computation, we have $T(0;\alpha,\beta,\lambda,\mu)=P_0=B(0)$, $T(1;\alpha,\beta,\lambda,\mu)=P_3=B(1)$, $B(1/2)-P^*=(1/8)(P_0-P_1-P_2+P_3)$, and

$$\begin{aligned}
T\left(\frac{\pi}{4};\alpha,\beta,\lambda,\mu\right)-P^*&=\left(1-\frac{\sqrt{2}}{2}\right)^{\alpha}\left(1-\lambda\frac{\sqrt{2}}{2}\right)(P_0\\
&-P_1)+\left(1-\frac{\sqrt{2}}{2}\right)^{\beta}\left(1-\mu\frac{\sqrt{2}}{2}\right)(P_3-P_2)\\
&\le\max\left\{8\left(1-\frac{\sqrt{2}}{2}\right)^{\alpha}\left(1-\lambda\frac{\sqrt{2}}{2}\right),8\left(1-\frac{\sqrt{2}}{2}\right)^{\beta}\right.\\
&\left.\cdot\left(1-\mu\frac{\sqrt{2}}{2}\right)\right\}\left[B\left(\frac{1}{2}\right)-P^*\right]\\
&=\max\left\{\phi\left(\alpha,\lambda\right),\varphi\left(\beta,\mu\right)\right\}\left[B\left(\frac{1}{2}\right)-P^*\right]\\
&=h\left(\alpha,\beta,\lambda,\mu\right)\left[B\left(\frac{1}{2}\right)-P^*\right].
\end{aligned}\tag{35}$$

These imply the theorem. □

From Theorem 6, we can see that TB-type curve $T((\pi/2)u;\alpha,\beta,\lambda,\mu)$ is closer to the control polygon than the cubic Bézier curve if $h(\alpha,\beta,\lambda,\mu)<1$. Figure 6 shows the comparison between the TB-type curves and the classical cubic Bézier curves under the same control points. It can be seen that as $\alpha=\beta$ increases at the same time, the resulting TB-type curves will be totally more close to the control polygon than the cubic Bézier curves. These indicate that the TB-type curves can better maintain the characteristic of the control polygon than the cubic Bézier curves.

Figure 7 shows the comparison between the TB-type curves and the polynomial Bézier curves with variable degree generated by the four polynomial Bernstein-like basis functions with variable degree given in the space spanned $\text{span}\{1,t,(1-t)^n,t^m\}$ given in [16] under the same control points. For the same degree, the TB-type curves have more computation complexity than the variable degree polynomial Bézier curves; however the resulting TB-type curves (solid lines) are nearer to the control polygon than the variable degree polynomial Bézier curves (dashed lines).

Figure 8 shows the comparison between the TB-type curves and the DTB-like curves generated by the four rational trigonometric basis functions constructed in the rational trigonometric space $\text{span}\{1,\sin^2 t,(1-\sin t)^2/[1+(\alpha-2)\sin t],(1-\cos t)^2/[1+(\beta-2)\cos t]\}$ given in [35] under the same control points. From Figure 8, clearly, the TB-type curves (solid lines) are closer to the control polygon than the DBT-like curves (dashed lines).

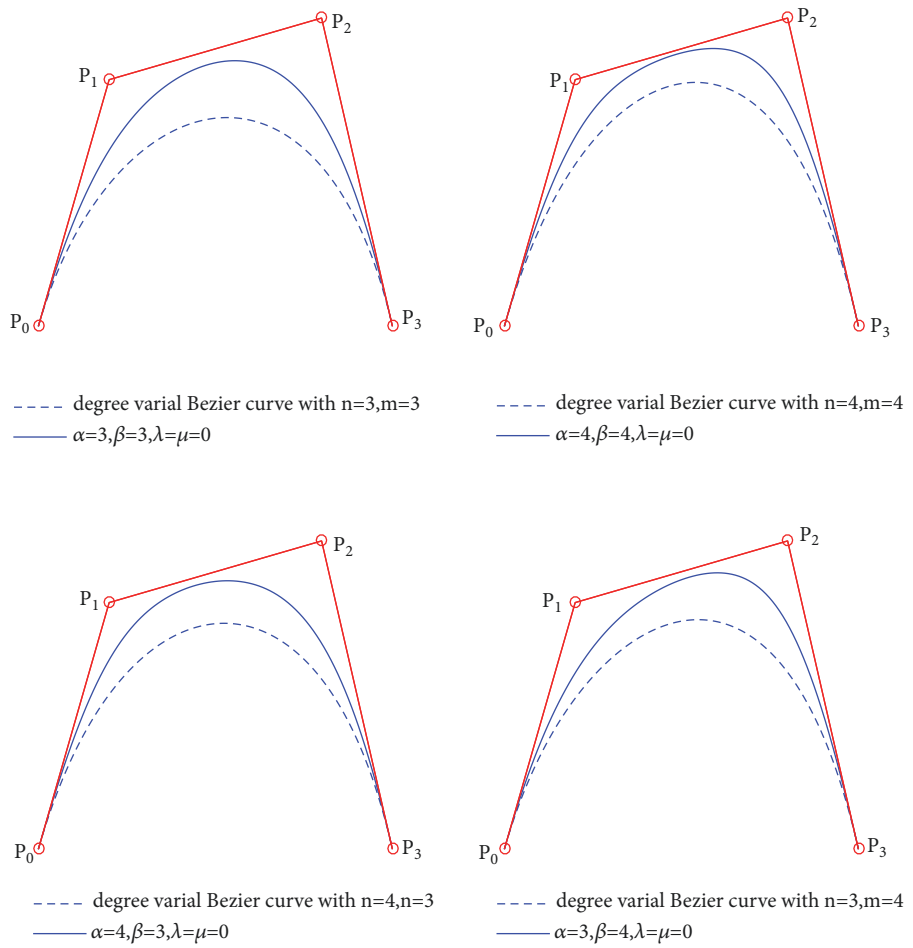

FIGURE 7: TB-type curves and variable degree polynomial Bézier curves.

3.4. Composite Trigonometric Bézier-Type Curves. In practical curve design, we often composite several TB-type curves to generate curves with complex shapes. In piecing TB-type curves together, we need to handle the smoothness connection conditions of the resulting curve. Give two TB-type curve segments as follows:

$$R_1(t;\alpha_1,\beta_1,\lambda_1,\mu_1)=\sum_{i=0}^{3}P_iT_i(t;\alpha_1,\beta_1,\lambda_1,\mu_1), \tag{36}$$

and

$$R_2(t;\alpha_2,\beta_2,\lambda_2,\mu_2)=\sum_{i=0}^{3}Q_iT_i(t;\alpha_2,\beta_2,\lambda_2,\mu_2). \tag{37}$$

It is obvious that if the point $P_3 = Q_0$, the two segments form a curve with C^0 continuity.

We shall derive some sufficient smoothness connection conditions for two TB-type curve segments forming a curve with C^1 or C^2 continuity. For knots $u_1 < u_2 < u_3$, we denote the resulting curve $R(u)$ constructed by (36) and (37) as follows:

$$R(u)=\begin{cases}R_1\left(\dfrac{\pi}{2}\cdot\dfrac{u-u_1}{h_1};\alpha_1,\beta_1,\lambda_1,\mu_1\right), & u\in[u_1,u_2],\\ R_2\left(\dfrac{\pi}{2}\cdot\dfrac{u-u_2}{h_2};\alpha_2,\beta_2,\lambda_2,\mu_2\right), & u\in[u_2,u_3],\end{cases} \tag{38}$$

where $h_i = u_{i+1} - u_i, i = 1, 2$.

Theorem 7. *For $\alpha_i, \beta_i \in [1, +\infty), i = 1, 2$, the resulting curve $R(u)$ is C^1 continuous at the knot u_2, if the following condition holds*

$$\begin{aligned}Q_0&=P_3,\\ Q_1&=\frac{(\beta_1+\mu_1)h_2}{(\alpha_2+\lambda_2)h_1}(P_3-P_2)+P_3.\end{aligned} \tag{39}$$

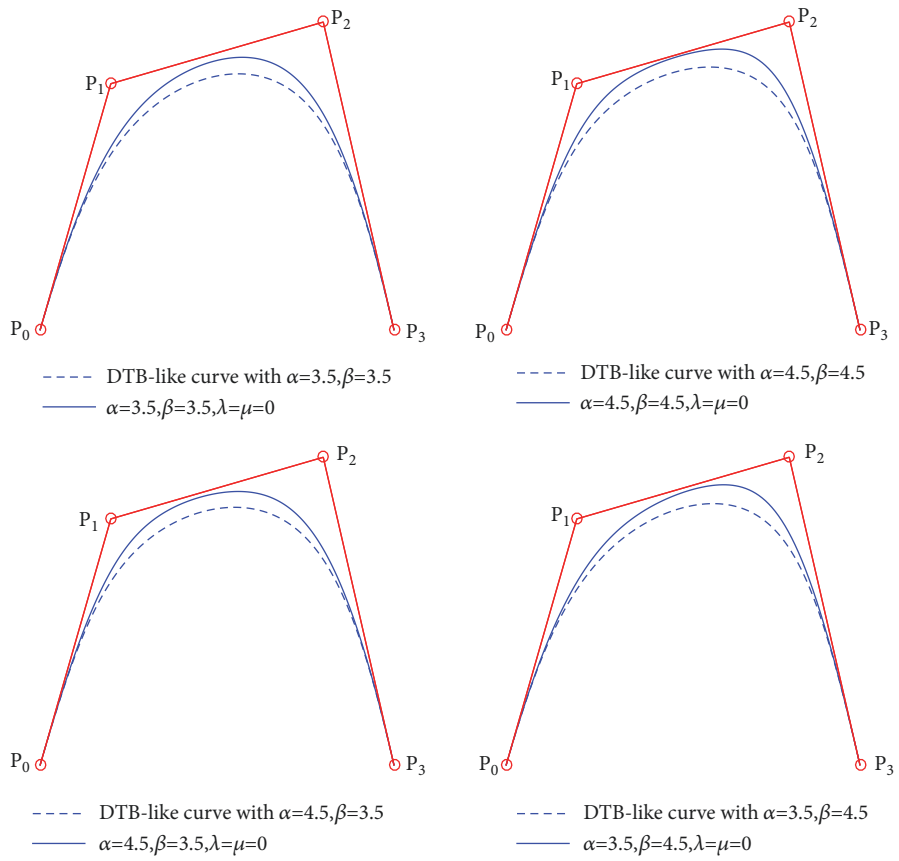

Figure 8: TB-type curves and DBT-like curves.

And for $\alpha_i, \beta_i \in (1, +\infty), i = 1, 2$, $R(u)$ is C^2 continuous at the knot u_2 if the condition (39) together with the following condition holds at the same time

$$Q_2 = \frac{h_2^2}{2h_1^2}\left[\left(\beta_1^2 + 2\mu_1\beta_1 - \beta_1\right)(P_3 - P_2) + 2(P_1 - P_2)\right] \tag{40}$$

$$+ \frac{1}{2}\left(\alpha_2^2 + 2\lambda_2\alpha_2 - \alpha_2\right)(Q_1 - Q_0) + Q_1. \tag{41}$$

Proof. After some direct computation, we get

$$R(u_2^-) = P_3,$$

$$R(u_2^+) = P_3,$$

$$R'(u_2^-) = \frac{\pi(\beta_1 + \mu_1)}{2h_1}(P_3 - P_2),$$

$$R'(u_2^+) = \frac{\pi(\alpha_2 + \lambda_2)}{2h_2}(Q_1 - Q_0),$$

$$R''(u_2^-) = \left(\frac{\pi}{2h_1}\right)^2 \cdot \left\{\left(\beta_1^2 + 2\mu_1\beta_1 - \beta_1\right)(P_3 - P_2) + 2(P_1 - P_2)\right\},$$

$$R''(u_2^+) = \left(\frac{\pi}{2h_2}\right)^2 \cdot \left\{\left(\alpha_2^2 + 2\lambda_2\alpha_2 - \alpha_2\right)(Q_0 - Q_1) + 2(Q_2 - Q_1)\right\}. \tag{42}$$

Thus under the conditions of Theorem 7, we can easily conclude the result. □

According to the end-point property of the TB-type curves given in (25), we can obtain the following interesting theorem.

Theorem 8. *For $h_1 = h_2 = h$, $\alpha_2 = \beta_1 \geq 2$, $\lambda_2 = \mu_1 \in (-\alpha_2, 1]$, $\alpha_1, \beta_2 \in [2, +\infty)$, $\lambda_1 \in (-\alpha_1, 1]$, $\mu_2 \in (-\beta_2, 1]$, if conditions (39) and (40) hold, then $R(u)$ will be C^3 continuous at the knot u_2. And for $h_1 = h_2 = h$, $\alpha_2 = \beta_1 = 3$, $\lambda_2 = \mu_1 = 0$, $\alpha_1, \beta_2 \in [3, +\infty)$, $\lambda_1 \in (-\alpha_1, 1]$, $\mu_2 \in (-\beta_2, 1]$, $R(u)$ will be C^5 continuous at the knot u_2 on condition that (39) and (40) hold.*

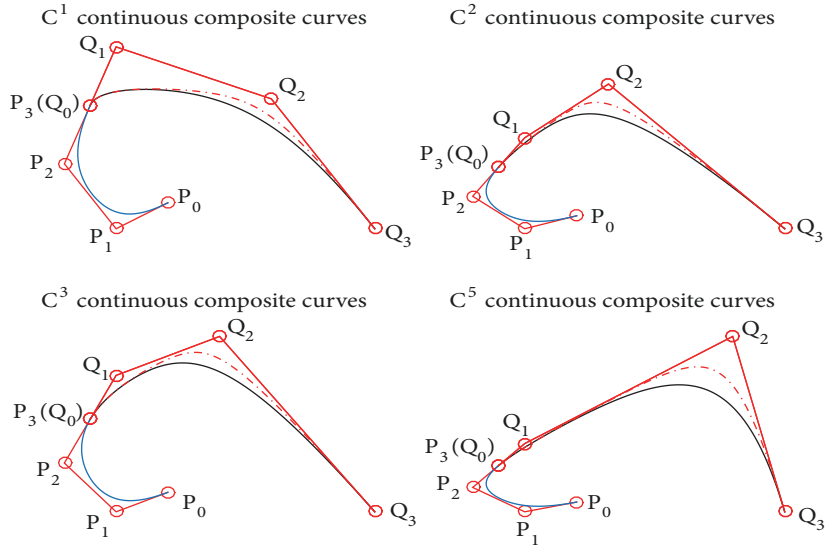

Figure 9: Composite TB-type curves.

Proof. For $h_1 = h_2 = h$, $\alpha_2 = \beta_1 \geq 2$, $\lambda_2 = \mu_1 \in (-\alpha_2, 1]$, $\alpha_1, \beta_2 \in [2, +\infty)$, $\lambda_1 \in (-\alpha_1, 1]$, $\mu_2 \in (-\beta_2, 1]$, from (39), we have

$$Q_1 - Q_0 = P_3 - P_2. \tag{43}$$

Straightforward computation gives that

$$\begin{aligned} R'''(u_2^-) &= \left(\frac{\pi}{2h}\right)^3 \\ &\cdot \left[\beta_1^3 + 3(\mu_1 - 1)\beta_1^2 - 3\mu_1\beta_1^2 + \beta_1 - \mu_1\right](P_3 - P_2), \\ R'''(u_2^+) &= \left(\frac{\pi}{2h}\right)^3 \\ &\cdot \left[\alpha_2^3 + 3(\lambda_2 - 1)\alpha_2^2 - 3\lambda_2\alpha_2 + \alpha_2 - \lambda_2\right] \\ &\cdot (Q_1 - Q_0). \end{aligned} \tag{44}$$

It follows that $R'''(u_2^+) = R'''(u_2^-)$.

Specially, for $h_1 = h_2 = h$, $\alpha_2 = \beta_1 = 3$, $\lambda_2 = \mu_1 = 0$, $\alpha_1, \beta_2 \in [3, +\infty)$, $\lambda_1 \in (-\alpha_1, 1]$, $\mu_2 \in (-\beta_2, 1]$, from (39) and (40), we have

$$\begin{aligned} Q_1 - Q_0 &= P_3 - P_2, \\ Q_2 - Q_1 &= (P_1 - P_2) + 6(P_3 - P_2). \end{aligned} \tag{45}$$

Direct computation gives that

$$\begin{aligned} R^{(4)}(u_2^+) &= \left(\frac{\pi}{2h}\right)^4 [24(Q_1 - Q_0) - 8(Q_2 - Q_1)], \\ R^{(4)}(u_2^-) &= \left(\frac{\pi}{2h}\right)^4 [-24(P_3 - P_2) + 8(P_2 - P_1)], \\ R^{(5)}(u_2^+) &= -57\left(\frac{\pi}{2h}\right)^5 (Q_1 - Q_0), \\ R^{(5)}(u_2^-) &= -57\left(\frac{\pi}{2h}\right)^5 (P_3 - P_2). \end{aligned} \tag{46}$$

Thus we have $R^{(4)}(u_2^+) = R^{(4)}(u_2^-)$, $R^{(5)}(u_2^+) = R^{(5)}(u_2^-)$. □

Figure 9 shows different smooth continuous composite TB-type curves. For C^1 continuous composite TB-type curves (blue curve and black curve), the shape parameters are $\alpha_1 = \beta_1 = 3$, $\alpha_2 = 1$, $\beta_2 = 3$, and $\lambda_1 = \mu_1 = \lambda_2 = \mu_2 = 0$. For C^2 continuous composite TB-type curves (blue curve and black curve), $\alpha_1 = \beta_1 = 3$, $\alpha_2 = 2$, $\beta_2 = 3$, and $\lambda_1 = \mu_1 = \lambda_2 = \mu_2 = 0$. For C^3 continuous composite TB-type curves (blue curve and black curve), $\alpha_1 = 3, \beta_1 = \alpha_2 = 2$, $\beta_2 = 3$, and $\lambda_1 = \mu_1 = \lambda_2 = \mu_2 = 0$. For C^5 continuous composite TB-type curves (blue curve and black curve), $\alpha_1 = 3$, $\beta_1 = \alpha_2 = 3$, $\beta_2 = 3$, and $\lambda_1 = \mu_1 = \lambda_2 = \mu_2 = 0$. From Theorems 7 and 8, it seems that the continuity of the resulting composite TB-type curves at the knot u_2 is related to the four shape parameters β_1, μ_1, α_2, and λ_2. Therefore, the shape of the resulting composite TB-type curves can be still modified by using the other four shape parameters α_1, λ_1, β_2, and μ_2 without changing the control points and the smoothness of composite TB-type curves. In Figure 9, the red dash-dotted curves are all generated by changing the shape parameter β_2 from 3 to 5. As a result, the resulting composite curves (blue curves and red dash-dotted curves) still maintain the same continuity at the knot u_2.

3.5. Tensor Product Trigonometric Bézier-Type Patches. From the univariate TB-type basis functions given in (19), we construct a class of tensor product trigonometric Bézier-type patches by using the classical tensor product method.

Definition 9. Given control points $P_{ij} \in \mathbb{R}^3 (i = 0, 1, 2, 3; j = 0, 1, 2, 3)$, we call

$$\begin{aligned} &S(u, v) \\ &= \sum_{i=0}^{3}\sum_{j=0}^{3} T_i(u; \alpha_1, \beta_1, \lambda_1, \mu_1)\, T_j(v; \alpha_2, \beta_2, \lambda_2, \mu_2)\, P_{ij}, \end{aligned} \tag{47}$$

$$0 \leq u, v \leq \frac{\pi}{2},$$

the tensor product trigonometric Bézier-type patch (TB-type patch for short) with eight shape parameters $\alpha_k, \beta_k, \lambda_k$, and $\mu_k, k = 1, 2$.

Since the univariate TB-type basis functions given in (19) can represent exactly arc of an ellipse or parabola, we expect that the associated TB-type patch can represent exactly ellipsoid patch and paraboloid patch if the control points and the shape parameters are chosen appropriately. In fact, suppose we choose control points of the TB-type patch as

$$\begin{aligned}
P_{00} &= (0, 0, c), \\
P_{01} &= (0, 0, c), \\
P_{02} &= (0, 0, c), \\
P_{03} &= (0, 0, c), \\
P_{10} &= \left(\frac{a}{2}, 0, c\right), \\
P_{11} &= \left(\frac{a}{2}, \frac{b}{4}, c\right), \\
P_{12} &= \left(\frac{a}{4}, \frac{b}{2}, c\right), \\
P_{13} &= \left(0, \frac{b}{2}, c\right), \\
P_{20} &= \left(a, 0, \frac{c}{2}\right), \\
P_{21} &= \left(a, \frac{b}{2}, \frac{c}{2}\right), \\
P_{22} &= \left(\frac{a}{2}, b, \frac{c}{2}\right), \\
P_{23} &= \left(0, b, \frac{c}{2}\right), \\
P_{30} &= (a, 0, 0), \\
P_{31} &= \left(a, \frac{b}{2}, 0\right), \\
P_{32} &= \left(\frac{a}{2}, b, 0\right), \\
P_{33} &= (0, b, 0),
\end{aligned} \tag{48}$$

in which $a, b, c > 0$, and take shape parameters $\alpha_1 = \alpha_2 = \beta_1 = \beta_2 = 2, \lambda_1 = \lambda_2 = \mu_1 = \mu_2 = 0$. Then from (47), we have

$$S(u, v) = \begin{bmatrix} x(u, v) \\ y(u, v) \\ z(u, v) \end{bmatrix} = \begin{pmatrix} a \sin u \cos v \\ b \sin u \sin v \\ c \cos u \end{pmatrix}, \quad 0 \le u, v \le \frac{\pi}{2}. \tag{49}$$

This expression indicates that $S(u, v)$ represent an ellipsoid patch. Obviously, if $a = b = c > 0$, then $S(u, v)$ represent a sphere patch.

Furthermore, for $\alpha_1 = \alpha_2 = \beta_1 = \beta_2 = 2$ and $\lambda_1 = \lambda_2 = \mu_1 = \mu_2 = 0$, if the control points with respective coordinates are as follows

$$\begin{aligned}
P_{00} &= \left(c, d, ac^2 + bd^2\right), \\
P_{01} &= \left(c, d, ac^2 + bd^2\right), \\
P_{02} &= \left(c, \frac{d}{2}, ac^2\right), \\
P_{03} &= \left(c, 0, ac^2\right), \\
P_{10} &= \left(c, d, ac^2 + bd^2\right), \\
P_{11} &= \left(c, d, ac^2 + bd^2\right), \\
P_{12} &= \left(c, \frac{d}{2}, ac^2\right), \\
P_{13} &= \left(c, 0, ac^2\right), \\
P_{20} &= \left(\frac{c}{2}, d, bd^2\right), \\
P_{21} &= \left(\frac{c}{2}, d, bd^2\right), \\
P_{22} &= \left(\frac{c}{2}, \frac{d}{2}, 0\right), \\
P_{23} &= \left(\frac{c}{2}, 0, 0\right), \\
P_{30} &= \left(0, d, bd^2\right), \\
P_{31} &= \left(0, d, bd^2\right), \\
P_{32} &= \left(0, \frac{d}{2}, 0\right), \\
P_{33} &= (0, 0, 0),
\end{aligned} \tag{50}$$

where $a, b, c, d \in \mathbb{R}$ and $c \cdot d \neq 0$, then from (47), we have

$$S(u, v) = \begin{bmatrix} x(u, v) \\ y(u, v) \\ z(u, v) \end{bmatrix} = \begin{pmatrix} \mathrm{c} \cos u \\ d \cos v \\ ac^2 \cos^2 u + bd^2 \cos^2 v \end{pmatrix}, \quad 0 \le u, v \le \frac{\pi}{2}. \tag{51}$$

This expression indicates that $S(u, v)$ represent a paraboloid patch: $z = ax^2 + by^2, 0 \le x/c \le 1, 0 \le y/d \le 1$.

Figure 10 shows an ellipsoid patch on left and a paraboloid patch on right. The ellipsoid patch is generated by setting the parameters $\alpha_1 = \alpha_2 = \beta_1 = \beta_2 = 2, \lambda_1 = \lambda_2 = \mu_1 = \mu_2 = 0$, and $a = 1, b = 2, c = 3$. And the paraboloid patch is generated by setting the parameters $\alpha_1 = \alpha_2 = \beta_1 = \beta_2 = 2, \lambda_1 = \lambda_2 = \mu_1 = \mu_2 = 0$, and $a = b = 2, c = d = 1$.

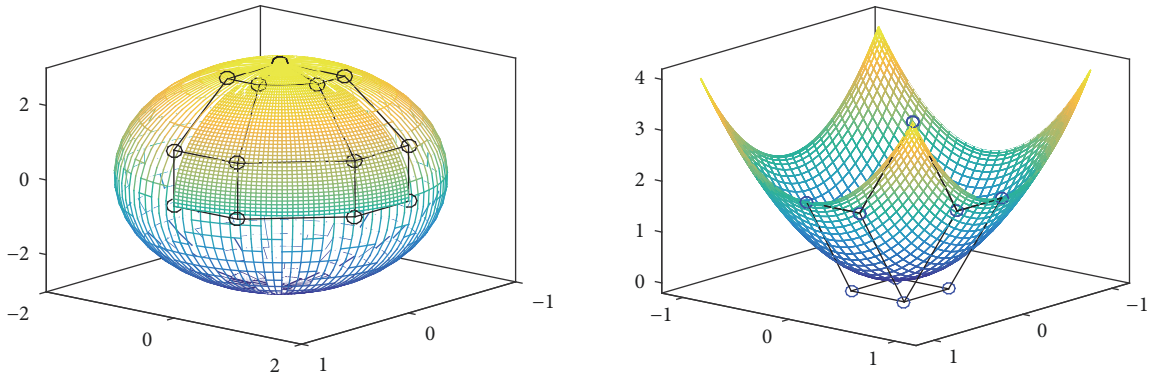

Figure 10: Reconstructed ellipsoid patch and paraboloid patch.

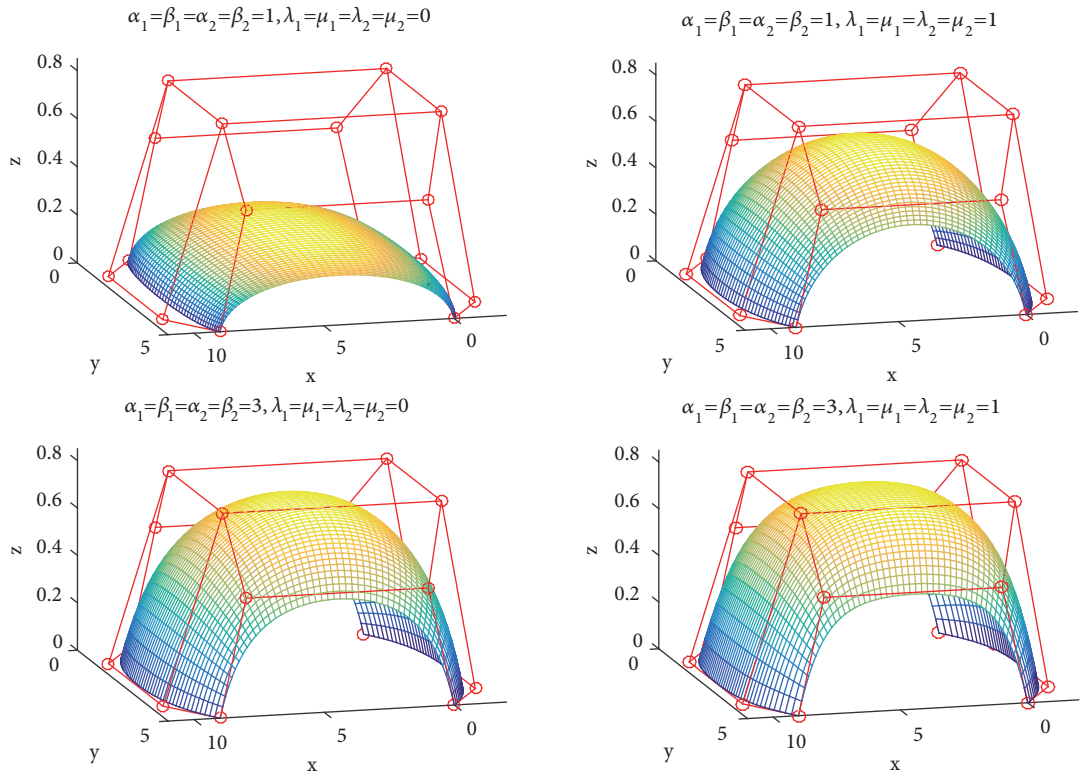

Figure 11: TB-type patches with different shape parameters.

Tensor product TB-type patches $S(u, v)$ have similar properties to that of TB-type curves given in (24) and we omit the details. Figure 11 shows some TB-type patches with different shape parameters under the fixed control points.

4. Conclusion

The four new developed trigonometric Bernstein-type basis functions with four shape parameters form a normalized basis with optimal total positivity and are useful for constructing parametric curves in CAGD, which include the bases given in [6–8, 34] as special cases. The four shape parameters have tension control property on modifying the shape of curves. By using the four shape parameters, the resulting trigonometric Bézier-type curves can be nearer to the given control polygon than the cubic Bézier curves. With appropriated choices of control points and shape parameters, any arc of an ellipse or parabola can be represented exactly by using the trigonometric Bézier-type curves. The new proposed corner cutting algorithm is useful for calculating the trigonometric Bézier-type curves efficiently and stably. There are also some work worthy of further study, such as subdivide algorithm for the new trigonometric Bézier-type curves. These will be our future work.

Data Availability

No data were used to support this study.

Conflicts of Interest

The authors declare that there are no conflicts of interest regarding the publication of this paper.

Acknowledgments

The research is supported by the National Natural Science Foundation of China (nos. 11771453, 61802129), the Postdoctoral Science Foundation of China (no. 2015M571931), the Fundamental Research Funds for the Central Universities (no. 2017MS121), and the Natural Science Foundation Guangdong Province, China (no. 2018A030310381).

References

[1] G. Farin, *Curves and Surfaces for Computer Aided Geometric Design*, Academic Press, San Diego, Calif, USA, 1993.

[2] L. Piegl and W. Tiller, *The NURBS Book*, Springer, New York, NY, USA, 1995.

[3] X. L. Han, "A class of general quartic spline curves with shape parameters," *Computer Aided Geometric Design*, vol. 28, no. 3, pp. 151–163, 2011.

[4] L. L. Yan and J. F. Liang, "An extension of the Bézier model," *Applied Mathematics and Computation*, vol. 218, no. 6, pp. 2863–2879, 2011.

[5] Y. P. Zhu and X. L. Han, "A class of spline curves with four local shape parameters," *Acta Mathematicae Applicatae Sinica*, vol. 33, no. 4, pp. 979–988, 2017.

[6] X. L. Han, "Cubic trigonometric polynomial curves with a shape parameter," *Computer Aided Geometric Design*, vol. 21, no. 6, pp. 535–548, 2004.

[7] X. Q. Wu, X. L. Han, and S. Luo, "Quadratic trigonometric polynomial Bézier curves with a shape parameter," *Journal of Engineering Graphics*, vol. 29, no. 4, pp. 82–87, 2008.

[8] X. A. Han, Y. C. Ma, and X. L. Huang, "The cubic trigonometric Bézier curve with two shape parameters," *Applied Mathematics Letters*, vol. 22, no. 2, pp. 226–231, 2009.

[9] X. A. Han, X. Huang, and Y. Ma, "Shape analysis of cubic trigonometric Bézier curves with a shape parameter," *Applied Mathematics and Computation*, vol. 217, no. 6, pp. 2527–2533, 2010.

[10] X. L. Han and Y. P. Zhu, "Total Positivity of the Cubic Trigonometric Bézier Basis," *Journal of Applied Mathematics*, vol. 2014, Article ID 198745, 5 pages, 2014.

[11] L. L. Yan, "Cubic trigonometric nonuniform spline curves and surfaces," *Mathematical Problems in Engineering*, vol. 2016, Article ID 7067408, 9 pages, 2016.

[12] J. W. Zhang, "C-curves: an extension of cubic curves," *Computer Aided Geometric Design*, vol. 13, no. 3, pp. 199–217, 1996.

[13] M. Hoffmann, Y. J. Li, and G. Z. Wang, "Paths of C-Bézier and C-B-Spline curves," *Computer Aided Geometric Design*, vol. 23, no. 5, pp. 463–475, 2006.

[14] J. M. Carnicer, E. Mainar, and J. M. Peña, "Critical length for design purposes and extended Chebyshev spaces," *Constructive Approximation*, vol. 20, no. 1, pp. 55–71, 2004.

[15] T. Bosner and M. Rogina, "Numerically stable algorithm for cycloidal splines," *Annali dell'Università di Ferrara. Sezione VII. Scienze Matematiche*, vol. 53, no. 2, pp. 189–197, 2007.

[16] P. Costantini, "Curve and surface construction using variable degree polynomial splines," *Computer Aided Geometric Design*, vol. 17, no. 5, pp. 419–446, 2000.

[17] M. L. Mazure, "Quasi-Chebyshev splines with connection matrices: application to variable degree polynomial splines," *Computer Aided Geometric Design*, vol. 18, no. 3, pp. 287–298, 2001.

[18] M. L. Mazure, "Blossoms and optimal bases," *Advances in Computational Mathematics*, vol. 20, no. 1-3, pp. 177–203, 2004.

[19] P. Costantini, T. Lyche, and C. Manni, "On a class of weak Tchebycheff systems," *Numerische Mathematik*, vol. 101, no. 2, pp. 333–354, 2005.

[20] M. L. Mazure, "On dimension elevation in quasi extended Chebyshev spaces," *Numerische Mathematik*, vol. 109, no. 3, pp. 459–475, 2008.

[21] M. L. Mazure, "Which spaces for design?" *Numerische Mathematik*, vol. 110, no. 3, pp. 357–392, 2008.

[22] M. L. Mazure, "On a general new class of quasi Chebyshevian splines," *Numerical Algorithms*, vol. 58, no. 3, pp. 399–438, 2011.

[23] M. L. Mazure, "Quasi extended Chebyshev spaces and weight functions," *Numerische Mathematik*, vol. 118, no. 1, pp. 79–108, 2011.

[24] T. Bosner and M. Rogina, "Variable degree polynomial splines are Chebyshev splines," *Advances in Computational Mathematics*, vol. 38, no. 2, pp. 383–400, 2013.

[25] P. Costantini and F. Pelosi, "Shape-preserving approximation by space curves," *Numerical Algorithms*, vol. 27, no. 3, pp. 219–316, 2001.

[26] P. Costantini and C. Manni, "Shape-preserving C3 interpolation: the curve case," *Advances in Computational Mathematics*, vol. 18, no. 1, pp. 41–63, 2003.

[27] P. Costantini and F. Pelosi, "Shape-preserving approximation of spatial data," *Advances in Computational Mathematics*, vol. 20, no. 1-3, pp. 25–51, 2004.

[28] W. Q. Shen, G. Z. Wang, and P. Yin, "Explicit representations of changeable degree spline basis functions," *Journal of Computational and Applied Mathematics*, vol. 238, pp. 39–50, 2013.

[29] X. L. Han and Y. P. Zhu, "Curve construction based on five trigonometric blending functions," *BIT Numerical Mathematics*, vol. 52, no. 4, pp. 953–979, 2012.

[30] M. Hoffmann, I. Juhasz, and G. Karosz, "A control point based curve with two exponential shape parameters," *BIT Numerical Mathematics*, vol. 54, no. 3, pp. 691–710, 2014.

[31] Y. P. Zhu and X. L. Han, "Curves and surfaces construction based on new basis with exponential functions," *Acta Applicandae Mathematicae*, vol. 129, pp. 183–203, 2014.

[32] Y. P. Zhu and X. L. Han, "New cubic rational basis with tension shape parameters," *Applied Mathematics-A Journal of Chinese Universities*, vol. 30, no. 3, pp. 273–298, 2015.

[33] Y. P. Zhu, "C2 rational quartic/cubic spline interpolant with shape constraints," *Results in Mathematics*, vol. 73, no. 3, pp. 73–127, 2018.

[34] Y. P. Zhu and X. L. Han, "New trigonometric basis possessing exponential shape parameters," *Journal of Computational Mathematics*, vol. 33, no. 6, pp. 642–684, 2015.

[35] K. Wang and G. C. Zhang, "New trigonometric basis possessing denominator shape parameters," *Mathematical Problems in Engineering*, vol. 2018, Article ID 9569834, 25 pages, 2018.